Supplementary information (ESI) for *Lab on a Chip*

Supplementary information: Experimental and model investigation of the time-dependent 2-dimensional distribution of binding in a herringbone microchannel

Jennifer O. Foley[a] Afshin Mashadi-Hossein[a,b] Elain Fu[a] Bruce Finlayson[c] and Paul Yager[a*]

Velocity profile in the herringbone microchannel

The model results for the velocity field of the herringbone microchannel (Figure 1) indicate that the velocity of the fluid within the herringbone was significantly lower than the velocity in the base microchannel. The velocity profile in the base microchannel closely resembles the parabolic velocity profile in the straight microchannel. However, unlike the uni-directional parabolic velocity profile in a straight microchannel, the velocity profile in a herringbone microchannel will have components in three dimensions (x-, y-, and z- dimensions instead of only the y-dimension). To understand the contribution of each component to the velocity field, the velocity fields in the x-, y-, and z-dimensions are shown for two different channel depths in Figure 2. The velocity profile near the binding surface is of particular importance to the surface binding profile of streptavidin.

In the herringbone microchannel, the fluid travels upward (x-dimension) to fill the herringbone microstructure and is then pushed downward toward the binding surface at the termination of the herringbone microstructure. This gives rise to an up and down motion in the velocity field (x-velocity profile in Figure 2). When the fluid first encounters the herringbone at the midline of the channel (z=250 microns), it moves rapidly into the herringbone microstructure (a positive velocity indicated in red) and away from the binding surface. At the terminus of the herringbone near the sidewalls of the microchannel, the fluid is pushed out of the herringbone and toward the binding surface (a negative velocity indicated in blue). In the rest of the microchannel, the x-velocity is minimal (near zero as indicated in turquoise). The x-velocity showed similar behavior near the binding surface (x=30 microns) and within the herringbone (x=110 microns).

The y-velocity profile near the binding surface (x=30 microns in Figure 2) varies down the length of the herringbone microchannel. The presence of the herringbone microstructures serves to increase the depth of the microchannel and therefore reduces the y-velocity in those locations (Figure 2; x=30 microns at locations demarked by the black arrows on the side of the microchannel). Within the herringbone microstructures (x=110 microns in Figure 2), the magnitude of the maximum y-velocity was ~4 times smaller than the velocity at x=30 microns (1.75×10^{-4} m/s versus 4.15×10^{-5} m/s). This is not unexpected as the general velocity field (Figure 1) indicates that the overall velocity is much lower within the herringbone microstructures than in the base microchannel. In the herringbone microstructure, the y-velocity is close to zero at the midline of the channel (z=250 microns), while the x-velocity is more dominant at that location. The y-velocity at the sidewalls of the herringbone microstructure is zero due to the no slip condition and the maximum y-velocity occurs at the center of the herringbone microstructure.

The herringbone microstructure induces a z-component in the velocity field (Figure 2). The magnitude of the velocity profile is symmetric about the midline of the channel (z=250 microns), where the z-velocity at both depths (x=30 microns and x=110 microns) is zero. Within the herringbone microstructure (x=110 microns in Figure 2), the fluid from the midline of the channel travels along the herringbone microstructure toward the sidewalls. Near the binding surface (x= 30 microns in Figure 2), the transverse velocity is highest in the smaller depth regions of the channel (i.e. where the herringbone microstructure is not present). The velocity profile indicates that the fluid travels from the sidewalls of the channel toward the center of the microchannel (i.e., in the opposite direction as in the herringbone microstructure). A more subtle result is that there exists some transverse flow before the fluid encounters the herringbones. This arises as fluid is pulled in the positive x-direction into the point of the herringbone microstructure at the midline of the microchannel (z=250 microns in Figure 2).

Combining the results for the x-, y-, and z-velocity profiles gives insight into the overall influence of the herringbone microchannel on the velocity profile. The results, which corroborate what has been presented elsewhere in the literature,[1] indicate that there is a circular nature to the convective flows within the herringbone microstructure. In each half of the herringbone microchannel, there exists rotation of the fluid (as qualitatively indicated in Figure 1 of the main article). In the upper half of the microchannel (z=250-500 microns), there is a counter-clockwise circulation (as viewed in the downstream direction). The fluid travels upward to fill the herringbone microstructure at the midline (x-velocity; z=250 microns), moves across the top of the herringbone towards the sidewalls (z-velocity), and is then pushed toward the binding surface at the sidewalls (x-velocity). Finally, the fluid flows toward the midline once the

[a] *Department of Bioengineering, University of Washington, Seattle, WA USA. Fax: 206-616-3928; Tel: 206-543-6126; E-mail: yagerp@u.washington.edu*
[b] *NanoString Technologies, Seattle, WA USA. Fax: 206-378-6288; Tel: 206-378-6288*
[c] *Department of Chemical Engineering, University of Washington, Seattle, WA USA. Fax: 206 685-3451; Tel: 206 685-1634;*

herringbone microstructure is terminated (z-velocity). Similarly on the bottom half of the microchannel (z=0-250 microns) there is a clockwise circulation of the fluid. In other words, at the midline of the channel (z=250 microns), the herringbone microstructure pulls the solution upward toward the top of the herringbone, across the top of the herringbone, down the sidewalls, and back across the binding surface. In the reverse herringbone microchannel, the direction of this recirculation is the reverse of the circulation pattern in the forward herringbone microchannel.

The number of turns per unit length of this rotation depends on the relative magnitudes of the y-velocity to the z-velocity. As the magnitudes of the velocities approach one another, the number of turns per unit length of the recirculation increases. In contrast, if the y-velocity is significantly larger than the z-velocity, the recirculation will travel down a much greater length of the channel before completing a rotation, resulting in fewer rotations per unit length.

Quantification of the relative contributions of the velocity components in the herringbone microchannel.

To gain a more quantitative understanding of the relative importance of each velocity component, two values were calculated. The first value, $D_n^{max\ or\ min}$ (Equation 1 and Table 1), is the maximum or minimum velocity in dimension n (x-, y- or z-dimension) divided by the average velocity in a straight microchannel. This value gives a sense of the relative importance of the maximum and minimum velocities in each dimension of the herringbone microchannel as compared to the average velocity in a straight microchannel. The data suggest that the magnitudes of the maximum and minimum x-velocities in the herringbone are significant, 43% and 34% of the average velocity of a straight microchannel. D_y^{max} was 158%, which was higher than expected as the maximum velocity in a straight microchannel is 150% of the average velocity. Detailed analysis of the y-velocity profiles indicated that the maximal velocity consistently occurred at the point of the first herringbone (data not shown), very near the midline of the channel (z ~250 micron; x ~90 micron). This maximal value could have arisen from the initialization of flow in directions besides the y-dimension or be attributed to numerical errors. The negative value for D_y^{min} is due to numerical artifacts and occurred in a small fraction of the microchannel, particularly near the walls and the outlet. The magnitudes of the maximal and minimal z-velocities in the herringbone are ~37% of the average velocity of a straight microchannel, indicating that significant transverse flows are generated locally within the microchannel. Furthermore, the fact that the maximum and minimum values were equal in magnitude are consistent with a symmetric flow profile in the z-dimension.

$$D_n^{\max\ or\ \min} = \left(\frac{v_n^{\max\ or\ \min\ of herringbone}}{v_{average}^{straight}} \right) \qquad \text{Equation 1}$$

The second value, F_n (Equation 2 and Table 2) is the fraction of total kinetic energy contributed by the velocity in dimension n (x-, y-, or z-dimension). Calculating the fractional contribution to the total kinetic energy by each velocity component gives a sense of the relative significance of each velocity component over the entire channel volume.

$$F_n = \int \left(\frac{v_n^2}{v_x^2 + v_y^2 + v_z^2} \right) dV \qquad \text{Equation 2}$$

The results (Table 2) indicate that the most significant contribution was due to the velocity component in the y-dimension at 98%. In contrast, the contribution due to the velocity component in the x-dimension was less than 1% and the contribution by the velocity in the z-dimension was ~1.3% of the total kinetic energy. These results corroborate the qualitative results presented in the image of the velocity field within the herringbone microchannel (Figure 1). As mentioned in the main article, the modeled and experimental herringbone geometries have not been optimized to achieve maximal transverse flow nor have they been optimized for maximal binding at the surface of interest. Therefore, it is expected that a significantly larger contribution by the z-component could be achieved from optimization of the herringbone geometry for this purpose.

Rectangular duct microchannel geometry

The rectangular duct microchannel (Figure 3), a structure in which ducts are positioned perpendicular to the y-dimension, above the base channel, was modeled with COMSOL and compared to herringbone and straight microchannels with comparable geometries and modeling conditions. The purpose of this model was to explore the influence of variation in the channel depth (x-dimension) on the streptavidin surface binding profile, independent of any angled geometric features.

The modeled flow rate was 5 nL/s. This corresponds to an average velocity of 1.11×10^{-4} m/s, a Reynolds number of 0.01, and a Peclet number of 135.1. The streptavidin concentration was 20 nM. The values of *w*, *d*, and *l* were the same for the straight, herringbone and rectangular duct microchannels (Figure 3). The values of *h* and *m* were the same for the herringbone and rectangular duct microchannels (Figure 3).

The varying depth of the rectangular duct microchannel (x-dimension) alters the local fluid velocity (Figure 4). In the base of the microchannel, the average velocity is highest in regions above which the duct is not present and lowest in regions above which a duct is present. The velocities within the ducts approach zero and are significantly lower than the velocity in the base of the microchannel.

The y-velocity (Figure 5) changes significantly as a result of the varying depth of the microchannel. The y-velocity is reduced in the regions of the base microchannel above which a duct is positioned (indicated by the black arrows at the side of the microchannel), and is increased in the regions of the base microchannel above which there is no duct. When fluid approaches a duct, the x-velocity is directed away from the binding surface (Figure 5) as the fluid travels to fill the duct (indicated in red). At the end of a duct, the fluid must travel out of the duct and the x-velocity is directed toward the binding surface (indicated in blue).

The values $D_n^{max\ or\ min}$ and F_n were calculated for the rectangular duct microchannel. The data suggests that D_x^{max}

is significant, ~25% of the average velocity of a straight microchannel. D_y^{max} is 152%, which is expected since the maximum velocity occurs in the smaller depth regions of the microchannel of the same dimension as the straight microchannel. The overshoot of two percent is within the error of the numerical simulation. A negative value for D_y^{min} could be due to a backward flow in the y- dimension in the top of the duct (data not shown) and previously reported in the literature.[1]

The results for F_n indicate that the velocity component in the y-dimension makes the largest contribution to the total kinetic energy, 99%. In contrast, the velocity component in the x-dimension contributes to only 1% of the total kinetic energy. This corroborates the qualitative results presented in the image of the velocity profile (Figure 5), in which the x-velocity is close to zero in most of the microchannel.

The surface binding profile of streptavidin to the biotin-functionalized surface over time (Figure 6) indicates that the binding profile varys with the depth of the microchannel. The smaller depth portions, where the fluid is moving faster, show increased binding. The model results indicate that the total amount of SA that binds to the surface over time does not differ between the rectangular duct, straight or herringbone microchannels (Figure 6 of the main article).

The bulk concentration profile of streptavidin in the microchannel (Figure 7) shows strong similarity to the concentration profile within a straight microchannel. Near the binding surface there is a significant depletion zone, and the depth of the depletion zone becomes slightly larger further downstream.

Notes and references

1 N. Jackson and B.A. Finlayson, *Journal of Non-Newtonian Fluid Mechanics*, 1982, **10**, 55.

Table 1 *D* values from model results. Normalized value of the maximum and minimum velocities in each dimension of the herringbone microchannel. Q=5 nL/s.

D_x^{max}	D_y^{max}	D_z^{max}	D_x^{min}	D_y^{min}	D_z^{min}
0.43	1.6	0.37	-0.34	-0.02	-0.37

Table 2 *F* values from model results. Fraction of kinetic energy due to the velocity in each dimension. Q=5 nL/s.

F_x	F_y	F_z
0.0060	0.98	0.013

Table 3 *D* values for the rectangular duct microchannel. Normalized value of the maximum and minimum velocities in each dimension calculated using model results.

D_x^{max}	D_y^{max}	D_x^{min}	D_y^{min}
0.25	1.5	-0.25	-0.08

Table 4 *F* values for the rectangular duct microchannel. Fraction of energy due to the velocity in each dimension calculated using model results.

F_x	F_y
0.0010	0.99

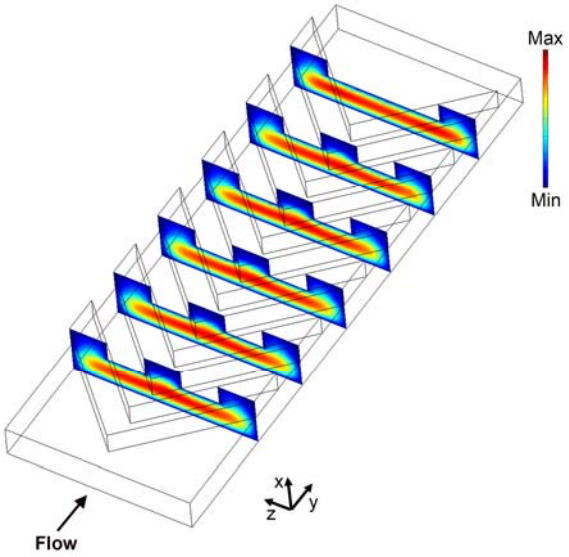

Fig. 1 Model results of the velocity profile (m/s) for a herringbone microchannel. The maximum velocity and minimum velocity were 1.74×10^{-4} m/s and 0 m/s, respectively.

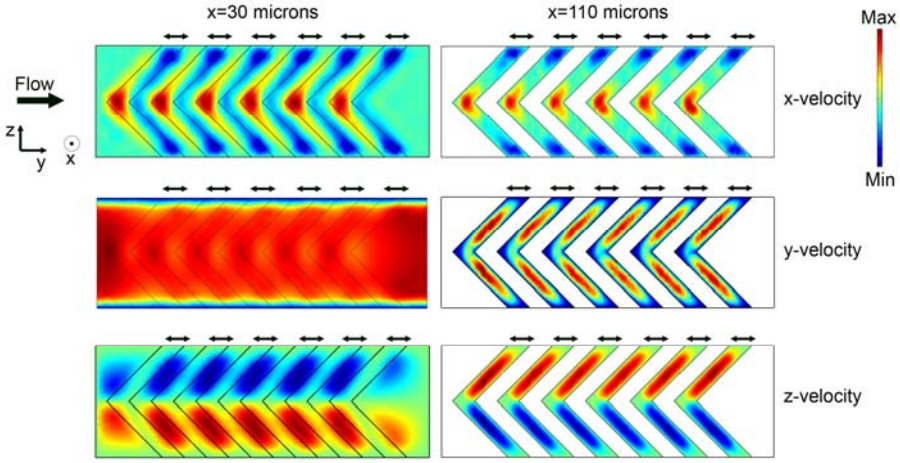

Fig.2 Model results of the x-, y-, and z-velocity profiles at two channel depths (x=30 microns, left, and x=110 microns, right) in a herringbone microchannel. The maximum and minimum x-velocities were 2.60×10^{-5} m/s and -2.07×10^{-5} m/s respectively, at x=30 microns. The maximum and minimum y-velocities were 1.75×10^{-4} m/s and -5.84×10^{-19} m/s respectively, at x=30 microns. The maximum and minimum z-velocities were 2.20×10^{-5} m/s and -2.21×10^{-5} m/s, respectively at x=30 microns. The maximum and minimum x-velocities were 1.44×10^{-5} m/s and -1.16×10^{-5} m/s, respectively at x=110 microns. The maximum and minimum y-velocities were 4.15×10^{-5} m/s and -8.66×10^{-19} m/s, respectively at x=110 microns. The maximum and minimum z-velocities were 4.10×10^{-5} m/s and -4.04×10^{-5} m/s, respectively at x=110 microns. The arrows indicate the deepest portion of the channel where the herringbone microstructure was present.

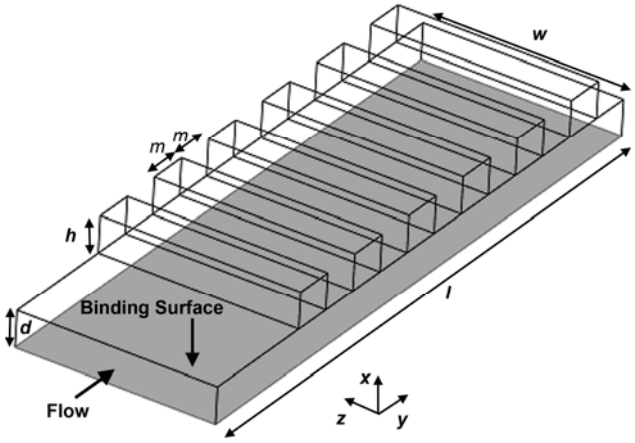

Fig. 3 Model geometry of the rectangular duct microchannel where *d*=90 microns, *h*= 90 microns, *w*=500 microns, *m*=100 microns, and *l*=1.5 mm. The streptavidin binding surface is indicated.

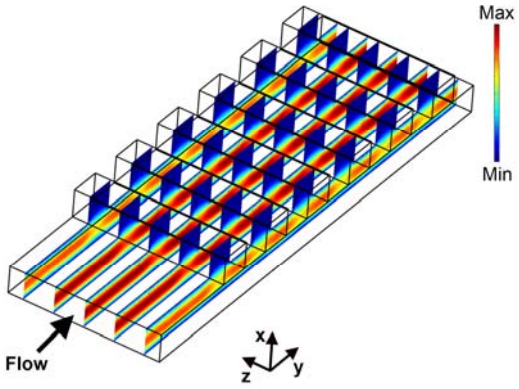

Fig. 4 Model results of the velocity profile (m/s) in the rectangular duct microchannel. The maximum and minimum velocities are 1.69×10^{-4} m/s and 0 m/s, respectively.

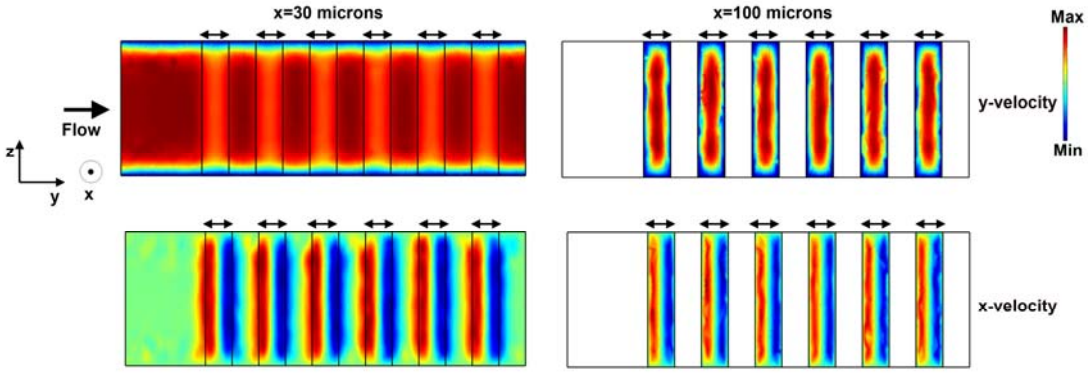

Fig. 5 Model results of the y-velocity and x-velocity profiles (m/s) in the rectangular duct microchannel at two channel depths, x=30 microns and x=100 microns. The arrows indicate the deepest portion of the channel where the rectangular duct structure is positioned above the base microchannel. The maximum and minimum y-velocities are 1.50×10^{-4} m/s and -4.73×10^{-19} m/s, respectively at x=30 microns. The maximum and minimum x-velocities are 9.54×10^{-6} m/s and -9.41×10^{-6} m/s, respectively at x=30 microns. The maximum and minimum y-velocities are 4.14×10^{-5} m/s and -9.15×10^{-6} m/s, respectively at x=100 microns. The maximum and minimum x-velocities are 2.00×10^{-5} m/s and -1.80×10^{-5} m/s, respectively at x=100 microns.

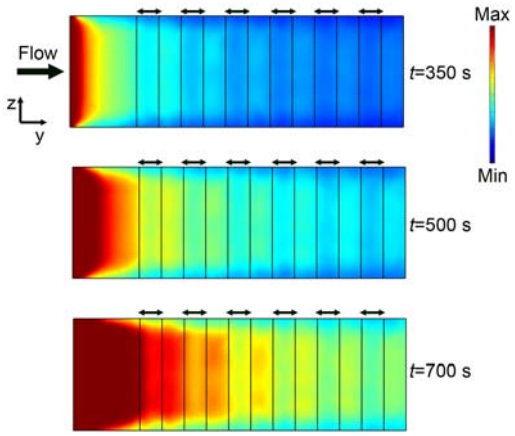

Fig. 6 Model results of the surface concentration profile of bound streptavidin (moles/m^2) in the rectangular duct microchannel. The arrows indicate the deepest portion of the channel where the rectangular structures are positioned above the base microchannel. The maximum surface binding concentration is 3.99×10^{-8} moles/m^2. The minimum surface binding concentration is 0 moles/m^2.The theoretical maximum surface binding concentration is 3.99×10^{-8} moles/m^2.

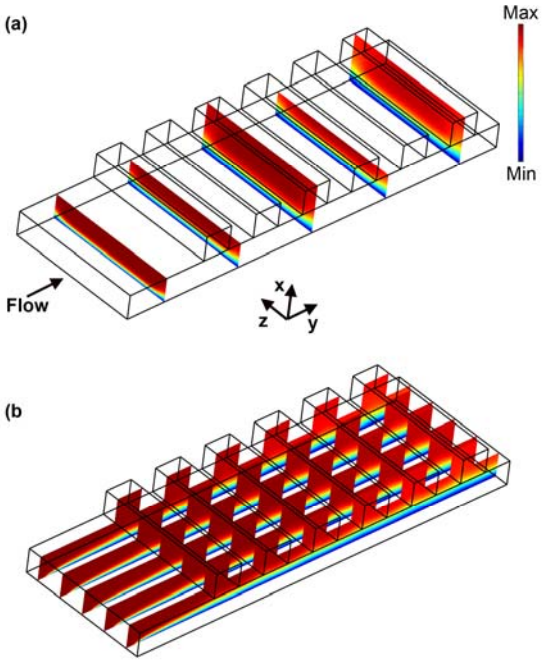

Fig. 7 Model results of the concentration profile of streptavidin in the rectangular duct microchannel channel. The maximum and minimum concentrations are 20 nM and 0 nM, respectively. Time = 350 seconds.